Published in final edited form as:
Sci Transl Med. 2012 January 18; 4(117): 117ra8. doi:10.1126/scitranslmed.3002670.

Normalization of Notch upregulation reverts large vessels to microvessels via EphB4-mediated venous reprogramming

Patrick A. Murphy[1,*,†], **Tyson N. Kim**[1,*], **Gloria Lu**[1], **Andrew W. Bollen**[2], **Chris B. Schaffer**[3], and **Rong A. Wang**[1]

[1]Laboratory for Accelerated Vascular Research, Division of Vascular Surgery, Department of Surgery, University of California, San Francisco

[2]Department of Pathology, University of California, San Francisco

[3]Department of Biomedical Engineering, Cornell University

Summary

High-flow through abnormal blood vessels underlies many life-threatening diseases. The ability to safely and non-invasively normalize these vessels by molecular intervention holds promise to treat these devastating conditions. Here we studied high-flow AV shunts caused by upregulation of Notch signaling via endothelial expression of constitutively-active Notch4 (*Notch4**). Using 4D, two-photon imaging with cellular resolution in live mice, we found that normalizing Notch signaling by turning off *Notch4** promptly converted large caliber, high-flow AV shunts to capillary-like vessels. The process was initiated by vessel narrowing without the loss of endothelial cells. Restoration of venous receptor EphB4 is an underlying mechanism, as EphB4 expression was recovered upon Notch normalization and required for the vessel regression. The structural regression of the high-flow AV shunts returned shunting flow to perfusing vessels, reversing tissue hypoxia and dysfunction. Our data provide direct, *in vivo* evidence that a single genetic manipulation in Notch pathway can exert dominant effects over hemodynamics leading to safe degeneration of the high-flow AV shunts at the core of AV Malformations.

Keywords

Arteriovenous malformation; Notch; Angiogenesis; Arterial Specification; Endothelial Cell; Stroke

Introduction

Abnormally enlarged high-flow vessels often continue to grow, leading to life-threatening ruptures. This dangerous vascular lesion underlies the pathology of a wide range of “high-flow” vascular diseases such as Arteriovenous Malformation (AVM), Hereditary Hemorrhagic Telangectasia (HHT) and Aneurysms (1). The hemodynamic stress exerted on the vasculature by these high-flow lesions can cause hemorrhagic rupture (1, 2). The ability to safely and non-invasively constrict the high-flow large vessels by molecular intervention holds promise to treat these life-threatening conditions that currently have limited effective treatments. We demonstrate here that established high-flow AV shunts can regress by a single genetic correction of Notch signaling.

*These authors contributed equally to this work
†Present address: Koch Institute for Integrative Cancer Research, Massachusetts Institute of Technology, Cambridge, MA 02139, USA

Normally, arteries carry blood from the heart to the capillaries, successively reducing vessel caliber and blood flow. Capillaries, where exchange of nutrients and wastes occurs, are the smallest diameter vessels with lowest blood flow. Post-capillary venules join sequentially wider veins to return blood back to the heart. This arterial-venous (AV) interface is critical for proper tissue perfusion. In AV shunts, the direct connection of arteries to veins displaces the perfusing capillaries, creating high-flow AV shunts that perpetuate lesion growth (2). Thus, high-flow AV shunts are the core defect in AVMs.

Notch receptors and ligands are transmembrane proteins that promote arterial at the expense of venous differentiation by enhancing expression of arterial molecular markers, such as *ephrinB2*, and suppressing the expression of venous markers, such as *EphB4* (3). The transmembrane signaling molecule *ephrinB2* was the first gene found to be expressed in the endothelial cells (ECs) of arteries and not veins, and is the most recognized arterial endothelial marker (4). Its cognate tyrosine kinase receptor, *EphB4*, was the first venous endothelial marker identified (4). *COUP-TFII*, a member of the orphan nuclear receptor superfamily expressed in venous and not arterial ECs, is upstream of *Notch* and actively promotes venous differentiation by repressing the expression of *Notch* (5). These AV specific genes are crucial in the morphogenesis of the embryonic vasculature, and their AV differential expression patterns persist in adult vascular endothelium (6, 7), suggesting post-natal retention of AV specification may have a role in maintaining vascular structure. Supporting this notion, we and others have reported that endothelial Notch activity is aberrantly increased in patients with brain AVMs (8, 9), supporting Notch signaling as a molecular lesion and a therapeutic target of this disease.

Here, using a mouse model of Notch-mediated AVM (10) and two-photon excited fluorescent imaging in live brains (11), we obtained 4D vascular topology and blood velocity data to demonstrate that high-flow AV shunts are remarkably reverted to capillary-like vessels after normalization of Notch, through an EphB4-dependent mechanism, without the loss of ECs.

Results

Repression of *Notch4** causes the specific regression of high-flow AV shunts

In our *Notch4*-Tet* mouse model of AVM, a constitutively-active Notch4 (*Notch4**) is specifically expressed in ECs, using a temporally-regulatable tetracycline (Tet)-repressible system (*Tie2-tTA; TRE-Notch4**) (12). Repression of Notch4* protein expression by Doxycycline (Dox) treatment was rapid, and approached baseline levels by 24hrs (Fig. S1). Since *Notch4** is rapidly repressed by Dox, we use *Notch4** repression instead of Dox treatment at times for clarity. *Notch4** expression leads to high-flow AV shunts in these mice. To directly test if these high-flow AV shunts normalize after the repression of *Notch4**, we combined two-photon microscopy with a cranial window placed over the right parietal cortex (Fig. S2) to visualize live brain vasculature over time.

To avoid the potential confounding effects of hemorrhage and animal illness in late stage, we focused on high-flow AV shunts at early stage, around postnatal day 12 (P12), when most mutants had just developed AV shunts. The minimum diameter of AV shunts at P11-13 averaged 22.2μm ± s.d. 7.3, ranging from 8.1 to 51.3μm (n=46 shunts in 13 mice), approximately 2 to 10 times the diameter of the capillaries in age-matched controls, which averaged 4μm ± s.d. 0.5, ranging from 2.7 to 5.0μm (n=9 capillaries in 3 mice, Fig. S3 & Table S1). Centerline flow velocity through AV shunts was much higher than in control capillaries, averaging 37.7mm/s ± s.d. 14.4 (n=11 shunts in 11 mice), compared to 2.1mm/s ± s.d. 1.0 in control capillaries (n=9 capillaries in 3 mice, Fig. S3 & Table S1), and as reported (13).

We then analyzed the diameter and flow in AV shunts before and after *Notch4** repression. We found that both diameter and flow were significantly decreased within 48hrs of Notch4* repression (Fig. 1), relative to untreated mutants (Fig. S4). Diameter changed primarily in the AV shunt and distal vein, adjacent arterial vessels were less affected (Fig. 1). To determine whether advanced AVM also regressed when Notch4* was turned off, we examined severely affected, ataxic mice at a later time point (P22), and found that these mature AVM also did regress (Fig. S5).

Not all AV shunts enlarge with continued *Notch4** expression, a variability likely caused by systemic hemodynamic instability. Therefore, we sought to identify a subset of "growth-prone" AV shunts to further test the effects of Notch4* repression. We found that among a "growth-prone" population of AV shunts, defined by continued growth over several days, all were induced to regress by *Notch4** repression (Fig. S6, 10 AV shunts in 8 mice). In contrast, without treatment, all of this population continued to grow (5 AV shunts in 2 mice).

When imaging for >1 week was possible, we observed the complete regression of the AV shunt to capillary diameter (Fig. S7), a finding also confirmed by *ex vivo* analysis (Fig. S7). Structurally, this regression involved the normalization of smooth muscle cell coverage (Fig. S8). Narrow time-point analysis indicated that the onset of diameter and velocity reductions coincided and occurred within 12–24hrs of *Notch4** repression (Fig. S9). Thus, our data shows that Notch4* repression results in the prompt narrowing of high-flow AV shunts.

*Notch4** repression directly induces narrowing of AV shunts

Since reductions in blood flow are known to cause vessel regression (14), we asked whether *Notch4** repression leads to shunt regression directly, or indirectly through the reduction of AV shunt flow. To discriminate between these possibilities, we measured blood flow in the upstream feeding artery, the AV shunt, and an adjacent artery.

If *Notch4** repression directly reduces the diameter of the AV shunt, we would expect increased resistance and decreased flow through the AV shunt (Fig. 2D). Consequently, the total flow through the feeding artery would also be reduced. Furthermore, the AV shunt blood flow would redistribute to adjacent arteries, thus increasing blood flow in adjacent arteries. Our empirical measurements matched these predictions; total blood flow was reduced, but flow through an adjacent artery to the AV shunt was increased (Fig. 2A–C).

Hypothetically, regression of the AV shunt might also be caused indirectly by the effects of reduced flow in the AV shunt following *Notch4** repression (Fig. 2D). Two possible scenarios might lead to reduced flow in the AV shunt. In one, resistance in the adjacent artery is reduced, "stealing" blood flow from the AV shunt. However, in this scenario, total systemic resistance to flow should also be reduced, and thus combined flow through the AV shunt and the adjacent artery should be increased, which we do not see. In a second scenario, systemic flow is reduced by events either upstream or downstream of the AV shunt and adjacent artery. However, in this scenario, flow through both the AV shunt and the adjacent artery should be reduced, which we also do not see. Thus, our data supports a direct mechanism for AV shunt regression following *Notch4** repression.

Vessel regression was initiated through a mechanism without the loss of endothelial cells

To understand the cellular mechanism of AV shunt regression, we asked whether reduction in the total number of ECs or the area covered by individual ECs was involved. To this end, we used the *ephrin-B2-H2B-eGFP* mouse line to provide nuclear labeling of ECs within the AV shunt (10). In the presence of *Notch4**, ECs in the AV shunt, regardless of arterial or venous origin, expressed *ephrin-B2-H2B-eGFP*. The H2B-eGFP fusion protein is extremely

stable and can persist for months (15). Thus, within the AV shunt, in the short time-frame of examination, *ephrin-B2-H2B-eGFP* serves as a general EC marker without arterial specificity.

We performed 4D imaging of AV shunt diameters and cell numbers in 23 AV shunts in seven *Tie2-tTA;TRE-Notch4*;ephrin-B2-H2B-eGFP* mice, at timepoints up to 48hrs following Notch4* repression. We found that all shunts regressed by 40 ± s.d. 14% by the 24 or 28hr timepoint. The onset of AV shunt regression was variable, sometimes occurring as early as 12hrs after Notch4* repression. Approximately 70% (18/23) of these AV shunts regressed without detectable loss of cells at 24 or 28hrs, judged by counting the eGFP+ nuclei. Fig. 3A shows such an example, where AV shunt regression was detected between 20–28hrs, and cell count was not reduced in the regressing AV shunts by 28hrs, nor by 36hrs with further vessel regression. Fig. S10 is another example. These results suggest that the AV shunt regression did not depend on the loss of vascular cells. We confirmed this hypothesis with an alternative method of tracking endothelial nuclei, using our *Tie2-tTA* induction system in conjunction with a *TRE-H2B-eGFP* reporter. We first verified that this reporter is a specific and robust marker of endothelial nuclei, as analysis of cell labeling in section revealed that 91.4 ± s.e.m. 3.4% of DAPI+ ECs, and none of the adjacent mural cells, were GFP+ (Fig. S11). We then analyzed vessel diameter and EC number up to 36hrs following Notch4* repression. By 12hrs, we detected regression in 36 of 38 AV shunts from 4 mice examined. Only 9 of the 36 regressing AV shunts exhibited loss of ECs. 27 AV shunts regressed without detectable loss of ECs (Fig. S12B). We did detect ECs loss later (Fig. S12B), after AV shunt regression, but this was not clearly correlated with either shunt diameter or degree of regression (Fig. S12C&D). Fig 3B depicts such an example, where AV shunt regression was detected between 12–20hrs, but cell count was not reduced until 36hrs following Notch4* repression. These data suggested that the initiation of AV shunt regression does not require the loss of ECs.

Ex vivo staining of VE-cadherin showing cell-cell junctions in mutants before and after repression of *Notch4** suggests that the area encompassed by individual ECs was reduced during regression (Fig. S13). Therefore, mean area, but not the total number, of ECs was reduced in the acute regression of AV shunts after *Notch4** repression.

Coup-TFII expressing venous endothelium within AV shunts upregulates EphB4 following repression of *Notch4**

We then asked whether recovery of venous specification, which was repressed in the presence of *Notch4**, might underlie the regression. *Coup-TFII* is a venous marker upstream of Notch. Therefore, we hypothesized that *Coup-TFII* expression would be retained in the cells of venous origin in the AV shunt, making it possible to trace the original venous segment and to assess the reestablishment of venous specification upon Notch4* repression. To determine *Coup-TFII* expression, we used a nuclear *lacZ* reporter of *Coup-TFII* promoter activity, *Coup-TFII*$^{+/fl\text{-}stop\text{-}nLacZ}$;*Tie2-Cre* (5). The *lacZ* expression is controlled by a floxed-STOP sequence. *Tie2-Cre*-mediated excision ensures that the *lacZ* reports the expression of *Coup-TFII* in *Tie2+* endothelial and hematopoetic cell lineages.

In the control, the *Coup-TFII* expression was localized to the endothelial nuclei of the venous branches, including capillaries, but absent in the arterial branches in the brain (Fig. 4A). In *Notch4** mutants (Fig. 4B&C), regardless whether *Notch4** was ON or OFF, *Coup-TFII* expression was maintained throughout the venous branches, as in controls. Thus, *Coup-TFII* expression clearly marked the venous boundary of AV shunts and suggests that part of the AV shunts originated from the vein.

EphB4, in contrast to *Coup-TFII*, is a Notch downstream venous marker (4, 16), making it possible to trace the effect of *Notch4** on venous repression. We used a *lacZ* reporter of *EphB4* promoter activity (16) to examine *EphB4* expression before and after *Notch4** repression. In controls, $EphB4^{tau\text{-}lacZ}$ was expressed throughout the veins, venules, and into the capillaries of the brains (Fig. 4D). *Notch4** expression decreased the expression of $EphB4^{tau\text{-}lacZ}$, resulting in patchy expression in the vein and very little expression in AV shunts (Fig. 4E).

To examine arterial marker expression during regression, we used an ephrin-B2 reporter. We have previously shown that ephrin-B2 expression is upregulated through the AV shunt in Notch4*-On mutants (10). Here, using $Ephrin\text{-}B2^{tau\text{-}lacZ}$ reporter mice, we confirmed this upregulation (Fig. 4H) and show ephrin-B2 was normalized when Notch4* was turned off (Fig. 4I). To determine whether Notch4* repression leads to the normalization of a broader arterial specification program in the AV shunts, we examined the expression of additional arterial specific proteins Dll4, Jag1, and Cx40 (Fig. 4J–U). We found that all of these genes were expressed preferentially in the arteries in controls, extended through AV shunts and veins when Notch4* was on in mutants, and normalized when Notch4* was turned off.

These data combined with the *Coup-TFII* expression pattern suggest that *Notch4** induced arterial identity and repressed venous identity in the venous segment. Repression of *Notch4** resulted in the loss of arterial markers ephrin-B2, Dll4, Jag1 and Cx40 (Fig. 4I,O,R,U) with a concomitant increase in *EphB4* expression in the regressing AV shunts (Fig. 4F).

To determine whether *EphB4* was re-expressed at the cellular level, we used the *TRE-H2B-eGFP* reporter to mark ECs in *Tie2-tTA; TRE-Notch4*; TRE-H2B-eGFP* mice expressing *Notch4** transgenes by eGFP expression, (Fig. 5A). We found that EphB4 protein expression was repressed to ~50% of control levels in the *TRE-H2B-eGFP*+venous ECs of *Tie2-tTA; TRE-Notch4*; TRE-H2B-eGFP* mutants, relative to *Tie2-tTA; TRE-H2B-eGFP* controls. Once the Notch4* transgene was turned off, EphB4 expression normalized to control levels in the venous cell population.

Inhibition of EphB4 signaling impairs regression of AV shunts

To determine whether EphB4 signaling is necessary for the regression of AV shunts, we used a soluble form of the EphB4 receptor to competitively inhibit EphB4 receptor signaling (17) following repression of *Notch4** (Fig. 5B). If regression depends upon EphB4 signaling, the soluble EphB4 receptor (sEphB4) should inhibit the reduction in AV shunt diameter induced by suppression of *Notch4**. Indeed, the mean change in the diameter of AV shunts (−17.8% ± s.d. 24.1) was significantly reduced relative to mice not treated with sEphB4 (−47% ± s.d. 19.3). As a control for the recombinant protein treatment, we examined regression in mice injected with recombinant human fibronectin. The mean change in AV shunt diameter in these mice (35.1% ± s.d. 26.2) was not significantly different from the regression in mice without recombinant protein treatment ($P<0.05$). Thus, sEphB4 significantly impaired the regression of AV shunts.

Regression of AV shunts alleviates hypoxia

To investigate the functional effect of AV shunt regression, we asked whether AV shunt regression reversed vascular dysfunction. We first examined blood velocity in arterial branches adjacent to the AV shunt and found blood velocity increased with *Notch4** repression but decreased with continued *Notch4** expression (Fig. 2C). Strikingly, these decreasing velocities could be promptly increased by *Notch4** repression and shunt regression (Fig. S6). Lectin perfusion of capillary vessels (Fig. 6A–C) suggests that tissue perfusion was globally increased following AV shunt regression.

We then examined hypoxia in *Notch4** mutants with neurologic defects before and after *Notch4** repression, using hypoxyprobe staining. Hypoxyprobe detects tissue exposed to a partial oxygen pressure of <10mmHg, close to the hypoxic threshold expected to cause dysfunction of neuronal cells (18). We detected an increase in hypoxyprobe staining in the cerebellum and cerebral cortex of sick *Notch4**-expressing mice, relative to their littermate controls (Fig. 6D&F). When *Notch4** was repressed for 72hrs in severely affected *Notch4** mutants, hypoxyprobe staining intensity was significantly reduced, and approached control levels (Fig. 6E).

Finally, we determined the histopathological changes in the brain parenchyma with and without *Notch4** repression. Histological analysis of *Notch4** mutants without *Notch4** repression revealed foci of pyknotic nuclei, often surrounding a core of decreased nuclear density, consistent with ischemia-induced necrosis (4 of 6 mice, Fig. 6G). Such regions occasionally also contained evidence of hemorrhage. *Notch4** repression for several weeks eliminated these pyknotic and acellular regions (9 of 9 mice), although structural damage could still be detected (Fig. 6H), presumably representing the evolution of the earlier ischemic damage. In support of this, hemosiderin depositions suggested the resolution of earlier hemorrhages. These findings suggest structural healing of earlier lesions after *Notch4** repression. Thus, regression of AV shunts induced by *Notch4** repression normalizes cerebrovascular flow patterns and tissue oxygenation, providing a physiologic explanation for recovered brain function.

Discussion

Here, we report that genetic reprogramming of AV specification converts high-flow AV shunts to low-flow microvessels. Using *in vivo* time-lapse imaging with single-cell resolution, we show that *Notch4** repression leads to a narrowing of AV shunts which does not require the loss of ECs, initiating AV shunt regression. Mechanistically, this involves the restoration of venous programming in the high-flow AV shunts by endothelial *Notch4** repression.

Notch induces reversible arterial programming of the venous compartment

Previously, we have observed expanded expression of the arterial marker *ephrin-B2* in the vasculature following upregulation of Notch signaling in mice (10, 12, 19). It is also reported that the arterial ECs in coronary artery development arise from venous vessels (20). However it is currently unknown whether venous ECs had been arterialized, or if arterial ECs had expanded. Using venous markers upstream (*Coup-TFII*) (5) and downstream (*EphB4*) (19) of Notch, we now show that Notch is sufficient to cause the arterialization of differentiated venous endothelium in the postnatal mouse. We show here, in normal brain endothelium, that *Coup-TFII* is preferentially expressed in venous and not arterial endothelium. Upstream of Notch, *Coup-TFII* expression is not affected by *Notch4** expression, identifying ECs of venous origin. Expression of *Notch4** led to the mis-expression of arterial markers ephrin-B2, Dll4, Jag1 and Cx40 in Coup-TFII positive veins, confirming that *Notch4** expression converts venous ECs into arterial ECs. Expression of *Notch4** also led to the suppression of the venous marker *EphB4* in the Coup-TFII positive cells, demonstrating a simultaneous loss of venous expression in ECs of venous lineage. Besides AV marker expression, *Notch4**-converted venous segments also exhibit the features of arteries, including arterial structure and flow velocity. Thus, our data demonstrate that Notch is sufficient to genetically arterialize veins.

We further demonstrate that this arterialization of veins by Notch upregulation is reversible. *Notch4** repression led to re-expression of venous marker *EphB4* in *Coup-TFII* positive vessels, as well as structural and hemodynamic normalization. Thus, our results suggest that

venous vessels arterialized by *Notch4** were reverted upon repression of *Notch4**. The reversible arterial specification in post-natal vasculature suggests that AV lineage specification is genetically pliable, and a single genetic manipulation is sufficient to switch AV specification postnatally.

AV reprogramming elicits the narrowing of high-flow AV shunts without the loss of ECs

The mechanism underlying the regression of AV shunts following *Notch4** repression involves *ephrin-B2* and *EphB4*-mediated EC reorganization, rather than a reduction of EC number. While the role of *Eph/ephrin* signaling in the endothelium is not yet clear, our finding is consistent with the established functions of *ephrin-B2/EphB4* in regulating cell migration through repulsive cues (21). We think that once re-expressed in *Coup-TFII*+ ECs, *EphB4* mediates *ephrin-B2* signaling and elicits EC repulsion (Fig. 7). Supporting a critical role for *ephrin-B2/EphB4* signaling in this normalization process, the specific regression of vessels occurs at the AV interface, while the adjacent arteries often do not regress. Furthermore, the regression of AV shunts following *Notch4** repression can be blocked by sEphB4.

The loss-less mechanism of AV normalization following *Notch4** repression is distinct from the apoptotic mechanism of vessel regression following VEGF withdrawal. Microvessels in tumors and normal tissues regress following VEGF inhibition (22). Regression in these vessels is attributed to apoptosis of ECs (23). Another model of vessel regression is the hyaloid vasculature of the eye (24). *In vivo* imaging of hyaloid vessel regression shows that the apoptosis of ECs obstructs the lumen and capillary blood flow, triggering the apoptosis of remaining ECs in the capillary segment and ultimately its regression (25). Thus, apoptosis and a subsequent reduction in blood flow are thought to precipitate vessel regression in these settings.

Our findings suggest that the cellular mechanism underlying the regression of the high-flow vessels following *Notch4** repression does not involve EC apoptosis, but likely EC reorganization.

Future implications

Our direct *in vivo* imaging demonstrates the regression of high-flow large vessels to capillary-like vessels by a single genetic manipulation. Strikingly, the vascular normalization was not accompanied by hemorrhage and vascular damage. Rather, AV shunt regression safely reversed tissue hypoxia and tissue dysfunction. We have focused on brain AVMs, but the finding likely applies to AVMs in other tissues, since we have previously identified *Notch4** mediated AVMs in the liver, skin, uterus and lung in the mouse (12, 19, 26). Thus, we believe that exploiting the tractable BAVM model system will provide important clues into the cellular and molecular regulation of AVMs in general. AV shunts are a core component of a range of “high-flow” vascular lesions (1). Thus, our demonstration of complete and safe normalization of dangerous high-flow AV shunts in animals may inspire molecular therapeutic strategies to induce the regression of these dangerous high-flow vessels and treat these devastating diseases.

Materials and Methods

Mice

Tie2-cre, *Tie2-tTA* and *TRE-Notch4** mice are published (8, 10, 12, 19), as are *Ephrin-B2*$^{+/H2B\text{-}eGFP}$ (27), *EphB4*$^{+/tau\text{-}lacZ}$ (16), *ephrin-B2*$^{+/tau\text{-}lacZ}$ (4), *mT/mG* (28), *TRE-H2B-eGFP* (29), and *Coup-TFII*$^{+/fl\text{-}stop\text{-}nLacZ}$ mice (30). Tetracycline solution (0.5 mg/ml Tet, 50 mg/ml sucrose, Sigma) was administered to mothers and withdrawn at birth (10).

Doxycycline treatment was initiated with intraperitoneal injection (500μL of 1 mg/mL in PBS), followed by doxycyline diet (200-mg/kg diet, Bio-Serv) (10, 12). All animals were treated in accordance with the guidelines of the University of California San Francisco Institutional Animal Care and Use Committee.

Soluble EphB4 treatment

200μL of 200μg/mL recombinant human EphB4 extracellular domain (R&D systems) was injected by tail vein (final concentration of ~4mg/kg), followed by 100μL of 200μg/mL 24hrs later (17). Recombinant human fibronectin (R&D systems) at the same concentration was a negative control.

In vivo imaging

Chronic *in vivo* brain vascular imaging was performed as described (11, 31), with modifications for immature mice (32). Briefly, a craniotomy was performed over the right cortex. A 5mm glass coverslip (World Precision Instruments) was placed over artificial cerebrospinal fluid and fixed into place. A custom metal bar was attached adjacent to the window, allowing it to be secured by a custom adaptor arm on a stereotaxic base (Cunningham). For imaging, mice were anesthetized with isoflurane (1.25–1.5%) in pure oxygen on homeothermic heat blanket (Harvard Apparatus). Fluorescent contrast agents were injected by tail vein [2000 kDa FITC-dextran (Sigma), 155 kDa TRITC-dextran (Sigma), or 2000 kDa Texas Red-dextran (prepared according to published protocols (33) and filtered by dialysis)]. Two-photon microscopy was performed with a locally constructed microscope, to be described in detail in a future publication.

Immunostaining

Conjugated *lycopersicon esculentum*-lectin (Vector Labs) was injected as we described (10, 12). Brain was fixed by 1% paraformaldehye (PFA) fixation via the left ventricle. Tissue was incubated in blocking solution (2% bovine serum albumin, 0.1% TritonX-100 in PBS), primary antibody overnight, and secondary antibody overnight. Antibodies were anti-VE-Cadherin (BD Pharminogen 555289, Clone 11D4.1, 1:200 dilution) and anti-α-SMactin (Sigma F377, Clone 1A4, 1:200 dilution) (12, 34). Staining for AV marker expression followed a similar protocol, except that blocking was with 10% donkey serum, 0.1% TritonX-100 in PBS. Antibodies (2ug/mL in block) were anti-Notch4-ICD (Millipore, 07–189), anti-Jag1 (R&D Systems BAF599), anti-Dll4 (R&D Systems, BAF1389), and anti-Cx40 (Santa Cruz, sc-20466).

Notch4 staining followed published protocols (10). Briefly, brains were perfusion-fixed with or without prior *lycopersicon esculentum*-lectin (Vector Labs) injection. After overnight fixation in 1% PFA, brains were sagittally bisected and dehydrated in 30% sucrose in PBS overnight and imbedded in OCT. 10μm sections were cut, blocked (3% donkey serum, 2% BSA, 0.2% TritonX-100 in PBS), and then incubated with anti-Notch4 ICD antibody (Millipore 07–189, formerly Upstate, 1:500 dilution) overnight in block, washed, incubated with secondary, washed and stored in VectaShield +DAPI (Vector Labs).

X-gal/DAB co-staining

Under ketamine/xylazine and isoflurane anesthesia, 25μg biotinylated *lycopersicon esculentum*-lectin (Vector Labs) was injected via inferior vena cava and allowed to circulate for 2 minutes. Perfusion was performed through the left ventricle with PBS, followed by fixative (0.25% gluteraldehyde, 50mM EGTA and 100mM MgCl2 in PBS). After short fixation, cortex was stained for beta-galactosidase at room temperature according to published X-gal protocols (35). Cortex was then fixed with 1% PFA, and blocked (10%

bovine serum albumin and 0.1% TritonX-100 in PBS), incubated with 1:1000 streptavidin conjugated horse-radish peroxidase (Jackson Immuno) in block, washed and stained with 3,3′-diaminobenzidine kit (Vector Labs).

Supplementary Material

Refer to Web version on PubMed Central for supplementary material.

Acknowledgments

We thank Claudia Tomas-Miranda and Dr. Weiya Jiang for experimental assistance, Dr. Sophia Tsai for the *Coup-TFII*$^{+/fl\text{-}stop\text{-}nLacZ}$ mice, Dr. Richard Daneman for critical reading, and members of our laboratory for helpful discussions. This work was supported by the Foundation for Accelerated Vascular Research (formerly the Pacific Vascular Research Foundation) and the Frank A. Campini Foundation, the Mildred V Strouss Trust, NIH R01 HL075033, NIH RO1 NS067420, and AHA Grant in Aid 10GRNT4170146 to R.A.W, and AHA 0715062Y and TRDRP 18DT-0009 Predoctoral Fellowships to P.A.M. and TRDRP 19DT- 007 and NIH F30 1F30HL099005-01A1 Predoctoral Fellowships to T.N.K.

References and Notes

1. Garzon MC, Huang JT, Enjolras O, Frieden IJ. Vascular malformations: Part I. J Am Acad Dermatol. Mar.2007 56:353. [PubMed: 17317485]
2. Friedlander RM. Clinical practice. Arteriovenous malformations of the brain. N Engl J Med. Jun 28.2007 356:2704. [PubMed: 17596605]
3. Roca C, Adams RH. Regulation of vascular morphogenesis by Notch signaling. Genes Dev. Oct 15.2007 21:2511. [PubMed: 17938237]
4. Wang HU, Chen ZF, Anderson DJ. Molecular distinction and angiogenic interaction between embryonic arteries and veins revealed by ephrin-B2 and its receptor Eph-B4. Cell. May 29.1998 93:741. [PubMed: 9630219]
5. You LR, et al. Suppression of Notch signalling by the COUP-TFII transcription factor regulates vein identity. Nature. May 5.2005 435:98. [PubMed: 15875024]
6. Shin D, et al. Expression of ephrinB2 identifies a stable genetic difference between arterial and venous vascular smooth muscle as well as endothelial cells, and marks subsets of microvessels at sites of adult neovascularization. Dev Biol. Feb 15.2001 230:139. [PubMed: 11161568]
7. Benedito R, Duarte A. Expression of Dll4 during mouse embryogenesis suggests multiple developmental roles. Gene Expr Patterns. Aug.2005 5:750. [PubMed: 15923152]
8. Murphy PA, Lu G, Shiah S, Bollen AW, Wang RA. Endothelial Notch signaling is upregulated in human brain arteriovenous malformations and a mouse model of the disease. Lab Invest. Sep.2009 89:971. [PubMed: 19546852]
9. ZhuGe Q, et al. Notch-1 signalling is activated in brain arteriovenous malformations in humans. Brain. Dec.2009 132:3231. [PubMed: 19812212]
10. Murphy PA, et al. Endothelial Notch4 signaling induces hallmarks of brain arteriovenous malformations in mice. Proc Natl Acad Sci USA. Aug 5.2008 105:10901. [PubMed: 18667694]
11. Schaffer CB, et al. Two-photon imaging of cortical surface microvessels reveals a robust redistribution in blood flow after vascular occlusion. PLoS Biol. Feb.2006 4:e22. [PubMed: 16379497]
12. Carlson TR, et al. Endothelial expression of constitutively active Notch4 elicits reversible arteriovenous malformations in adult mice. Proc Natl Acad Sci USA. Jul 12.2005 102:9884. [PubMed: 15994223]
13. Unekawa M, et al. RBC velocities in single capillaries of mouse and rat brains are the same, despite 10-fold difference in body size. Brain Res. Mar 12.1320:69. [PubMed: 20085754]
14. Jones EA, le Noble F, Eichmann A. What determines blood vessel structure? Genetic prespecification vs. hemodynamics. Physiology (Bethesda). Dec.2006 21:388. [PubMed: 17119151]

15. Fuchs E. The tortoise and the hair: slow-cycling cells in the stem cell race. Cell. May 29.2009 137:811. [PubMed: 19490891]
16. Gerety SS, Wang HU, Chen ZF, Anderson DJ. Symmetrical mutant phenotypes of the receptor EphB4 and its specific transmembrane ligand ephrin-B2 in cardiovascular development. Mol Cell. Sep.1999 4:403. [PubMed: 10518221]
17. Kertesz N, et al. The soluble extracellular domain of EphB4 (sEphB4) antagonizes EphB4-EphrinB2 interaction, modulates angiogenesis, and inhibits tumor growth. Blood. Mar 15.2006 107:2330. [PubMed: 16322467]
18. Rolett EL, et al. Critical oxygen tension in rat brain: a combined (31)P-NMR and EPR oximetry study. Am J Physiol Regul Integr Comp Physiol. Jul.2000 279:R9. [PubMed: 10896858]
19. Kim YH, et al. Artery and vein size is balanced by Notch and ephrin B2/EphB4 during angiogenesis. Development. Nov.2008 135:3755. [PubMed: 18952909]
20. Red-Horse K, Ueno H, Weissman IL, Krasnow MA. Coronary arteries form by developmental reprogramming of venous cells. Nature. Mar 25.464:549. [PubMed: 20336138]
21. Pitulescu ME, Adams RH. Eph/ephrin molecules--a hub for signaling and endocytosis. Genes Dev. Nov 15.24:2480. [PubMed: 21078817]
22. Jain RK. Normalization of tumor vasculature: an emerging concept in antiangiogenic therapy. Science. Jan 7.2005 307:58. [PubMed: 15637262]
23. Baffert F, et al. Cellular changes in normal blood capillaries undergoing regression after inhibition of VEGF signaling. Am J Physiol Heart Circ Physiol. Feb.2006 290:H547. [PubMed: 16172161]
24. Lobov IB, et al. WNT7b mediates macrophage-induced programmed cell death in patterning of the vasculature. Nature. Sep 15.2005 437:417. [PubMed: 16163358]
25. Meeson A, Palmer M, Calfon M, Lang R. A relationship between apoptosis and flow during programmed capillary regression is revealed by vital analysis. Development. Dec.1996 122:3929. [PubMed: 9012513]
26. Miniati D, et al. Constitutively active endothelial Notch4 causes lung arteriovenous shunts in mice. Am J Physiol Lung Cell Mol Physiol. Feb.298:L169. [PubMed: 19933399]
27. Davy A, Bush JO, Soriano P. Inhibition of gap junction communication at ectopic Eph/ephrin boundaries underlies craniofrontonasal syndrome. PLoS Biol. Oct.2006 4:e315. [PubMed: 16968134]
28. Muzumdar MD, Tasic B, Miyamichi K, Li L, Luo L. A global double-fluorescent Cre reporter mouse. Genesis. Sep.2007 45:593. [PubMed: 17868096]
29. Tumbar T, et al. Defining the epithelial stem cell niche in skin. Science. Jan 16.2004 303:359. [PubMed: 14671312]
30. Takamoto N, et al. COUP-TFII is essential for radial and anteroposterior patterning of the stomach. Development. May.2005 132:2179. [PubMed: 15829524]
31. Holtmaat A, et al. Long-term, high-resolution imaging in the mouse neocortex through a chronic cranial window. Nat Protoc. 2009; 4:1128. [PubMed: 19617885]
32. Portera-Cailliau C, Weimer RM, De Paola V, Caroni P, Svoboda K. Diverse modes of axon elaboration in the developing neocortex. PLoS Biol. Aug.2005 3:e272. [PubMed: 16026180]
33. Hornig S, et al. Biocompatible fluorescent nanoparticles for pH-sensoring. Soft Matter. 2008; 4:1169.
34. Braren R, et al. Endothelial FAK is essential for vascular network stability, cell survival, and lamellipodial formation. J Cell Biol. Jan 2.2006 172:151. [PubMed: 16391003]
35. Carpenter B, et al. VEGF is crucial for the hepatic vascular development required for lipoprotein uptake. Development. Jul.2005 132:3293. [PubMed: 15944181]

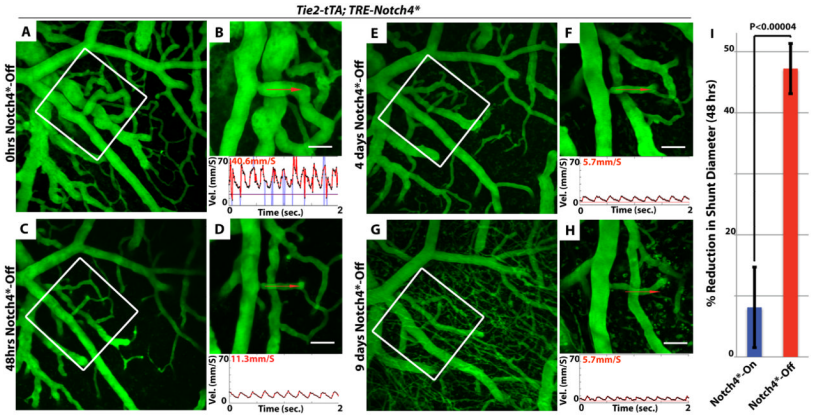

Figure 1. Repression of *Notch4 induces the normalization of arteriovenous malformation**

(A–H) Two-photon timelapse imaging of cortical brain vessels through a cranial window in *Notch4** mutant mice. Vessel topology was visualized by intravenous FITC-dextran. Arteriovenous shunt (A&B) was reduced in diameter following the repression of *Notch4** (C–H). Centerline velocity in the regressing AV shunt was obtained by direct measurement of the velocity of individual red blood cells (panels B,D,F,H). Repression of *Notch4** decreased blood flow velocity in shunt by 48hrs (compare B to D). (I) Quantification of the changes in shunt diameter without repression of *Notch4** (*Notch4**-On) or with repression of *Notch4** (*Notch4**-Off) for 48hrs. Diameter was measured at the narrowest point between artery and vein in *Notch4**-On mice before and after treatment (*n*=22 AV shunts in 10 mice with and *n* =35 AV shunts in 11 mice without *Notch4** repression). Error bars represent s.e.m. between individual AV shunts. Scale bars = 50μm.

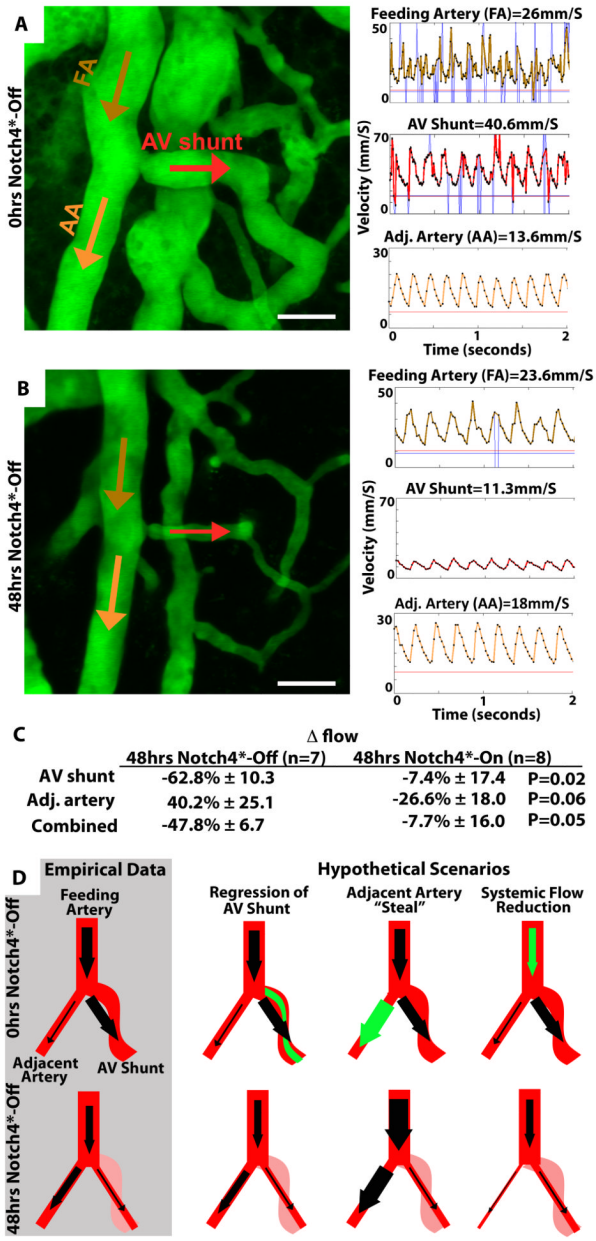

Figure 2. Flow analysis indicates that AVM narrowing is the primary event in AVM regression

(A&B) Two-photon timelapse imaging of cortical brain vessels through cranial window in *Notch4** mutant mice. Vessel topology was visualized by plasma labeling by intravenous FITC-dextran. Centerline velocity in the regressing AV shunt, feeding artery (FA) and adjacent artery (AA) was obtained by direct measurement of the velocity of individual red blood cells. Repression of *Notch4** decreased blood flow velocity by 48hrs in shunt and feeding artery, but increased velocity in adjacent artery. (C) Summary of % Δ in calculated flow in vessels either 48hrs after *Notch4** suppression or after 48hrs with no *Notch4** suppression. (D) Illustration of empirical data and hypothetical scenarios of regression. The primary event can be either the acute narrowing of the AV shunt or a reduction in flow, caused by either steal from an adjacent artery or a systemic reduction in flow. The acute AV shunt narrowing model, predicting the increase in adjacent artery flow and reduction in

feeding artery flow, best fits the empirical observations. We do not observe increased feeding artery flow, as predicted by the adjacent artery “steal” model, or a decrease in adjacent artery flow, as predicted by systemic flow reduction model. Scale bars = 50μm.

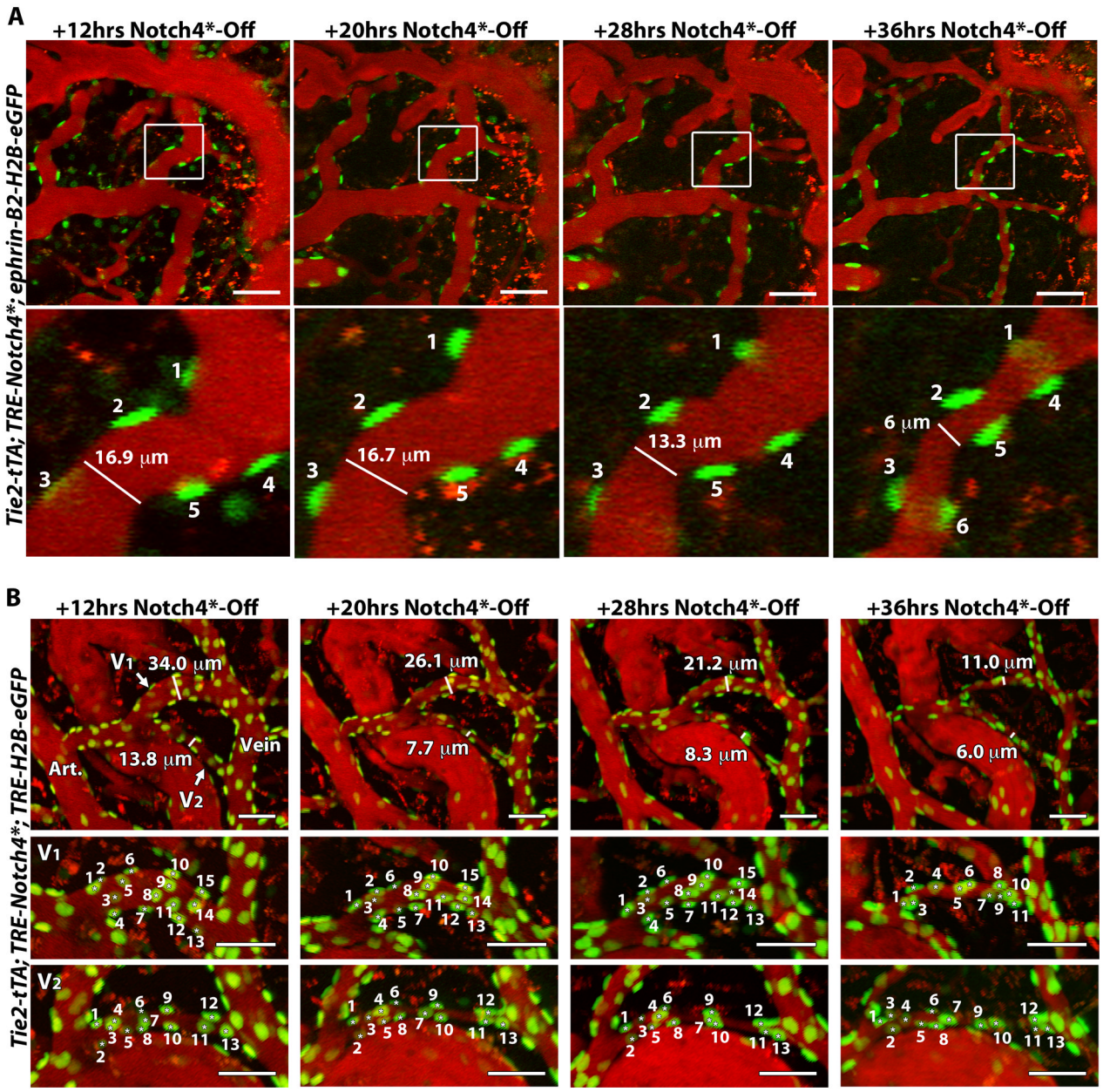

Figure 3. Regression is initiated by the loss-less reorganization of endothelial cells

(A) Two-photon timelapse imaging through a cranial window of nuclei marked by *ephrin-B2*$^{+/H2B\text{-}eGFP}$ in a *Notch4** mutant mouse. Plasma was labeled by intravenous Texas Red-dextran. In the AV shunt shown, vessel diameter was reduced by 28hrs after Notch4* repression, while the GFP+ nuclei, representing the cells, were retained at 28hrs, and even at 36hrs when vessel was further regressed. Because these images are Z-stacks through the vessel, cell 6 presented at 36hrs was also present earlier but out of the imaging plane. (B) Two-photon timelapse imaging through a cranial window of nuclei marked by *Tie2-tTA/TRE-GFP* in a Notch4* mutant mouse. Plasma was labeled by intravenous Texas Red-dextran. In the AV shunt shown, vessel diameter was reduced by 20hrs after Notch4* repression, while the GFP+ nuclei, representing ECs, were retained at 20hrs, and even at 28hrs when vessel was further regressed. At 36hrs further regression was evident, when

some loss of was detected in the large shunt, V1, but not the smaller shunt, V2. Scale bars = 50μm.

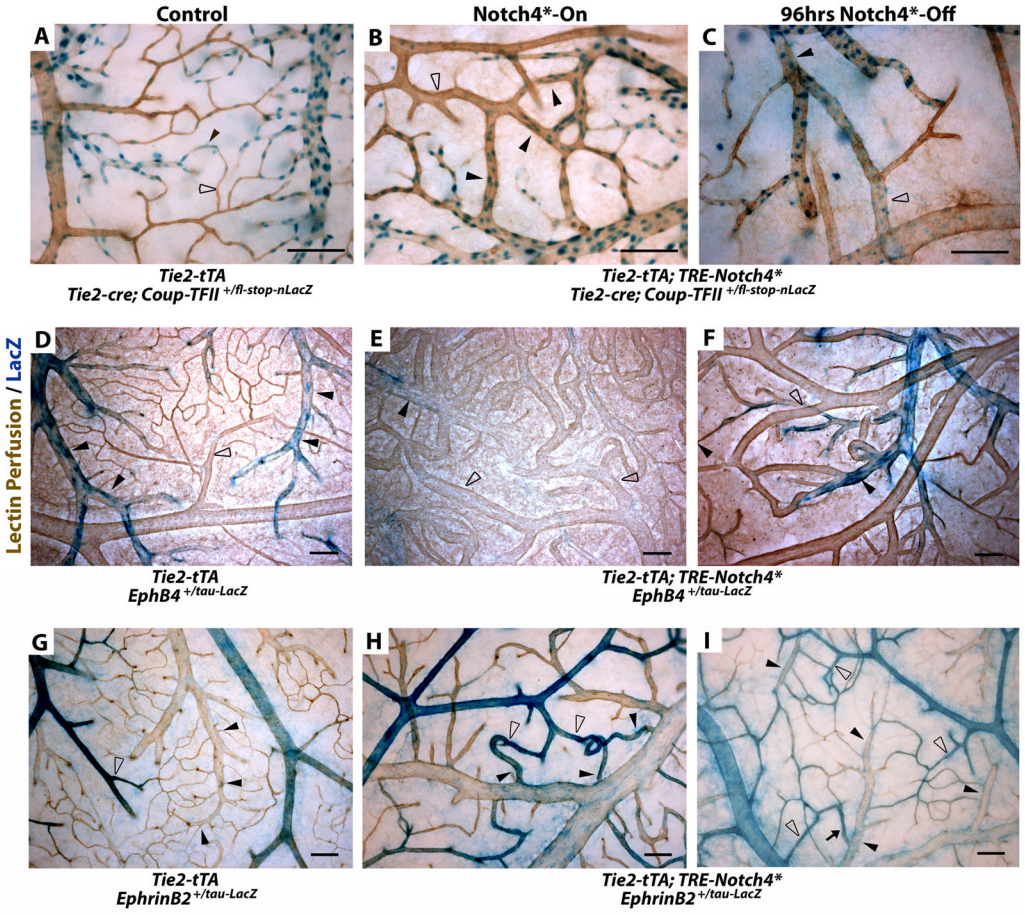

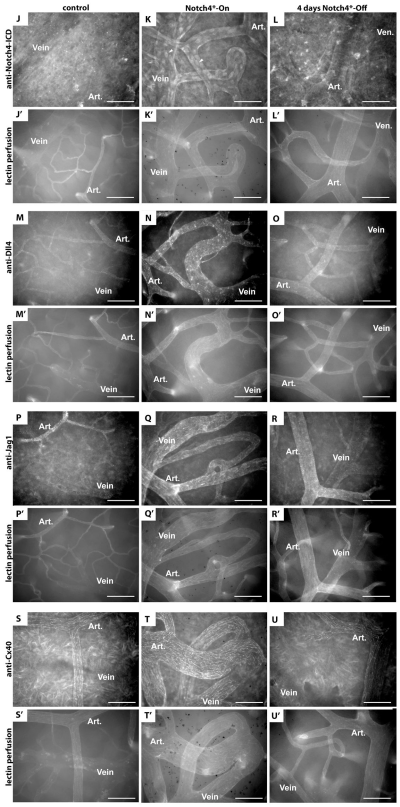

Figure 4. Turning off Notch4* normalizes arteriovenous specification in AV shunts

(A–I) Whole mount LacZ staining of the surface vasculature of the cerebral cortex to reveal expression of Notch upstream venous specification gene *Coup-TFII*, downstream venous marker *EphB4*, and downstream arterial marker *ephrin-B2*. Perfused vessels were counterstained by colorimetric 3,3′-diaminobenzidine (DAB) reaction with horseradish peroxidase (HRP) bound tomato-lectin. (A–C) LacZ staining of *Tie2-cre* activated *Coup-TFII* reporter. (A) In control mice, *Coup-TFII* was expressed in the veins, venules and capillaries up to the arterioles. (B) In *Notch4** expressing mutants, *Coup-TFII* was expressed in the vein, and venous portion of the AV shunt. (C) After repression of *Notch4**, the narrowest point in AV shunts was found between *Coup-TFII* positive and *Coup-TFII* negative endothelium. (D–F) LacZ staining of *EphB4* reporter. (D) In control mice, *EphB4* was expressed in the veins and venules up to the capillaries. (E) In *Notch4** expressing mutants, *EphB4* expression was reduced through AV shunts, venules and veins. (F) Following the repression of *Notch4**, *EphB4* expression was increased in the regressing AV shunt. (G) In control mice, *ephrin-B2* expression was detected in the arteries and arterioles up to the capillaries. (H) In *Notch4** expressing mutants, *ephrin-B2* expression was detected in arteries, the AV shunts, and at lower levels extending into the veins. (I) After repression of *Notch4**, *ephrin-B2* expression was decreased in the regressing AV shunts and veins. Closed arrowheads indicate venules; open arrowheads indicate arterioles. *n*=3 (A–C,G,I), *n*=4 (H), and *n*=8 (D–F) for each condition. Scale bars = 100μm.

(J–U) Whole mount immuno-fluorescence staining of cerebral cortex after FITC-lectin perfusion. (J–L) Endothelial localization of Notch4-ICD was undetectable in control mice (J), but present in a focal manner consistent with nuclear localization throughout the artery and vein in Notch4*-On mice (arrowheads in K), and reduced once Notch4* was turned off (L). Arterial markers Dll4 (M–O), Jag1 (P–R) and Cx40 (S–U) were expressed in the artery and not vein in control mice (M,P,S). All of these markers were upregulated in the artery,

through the AV shunt, and into the vein in Notch4*-On mice (N,Q,T). When Notch4* was turned off the expression in the AV shunt and vein was lost, but arterial expression remained (O,R,U). *n*=5 for all mutants, *n*=2 for each controls. Scale bars = 100μm.

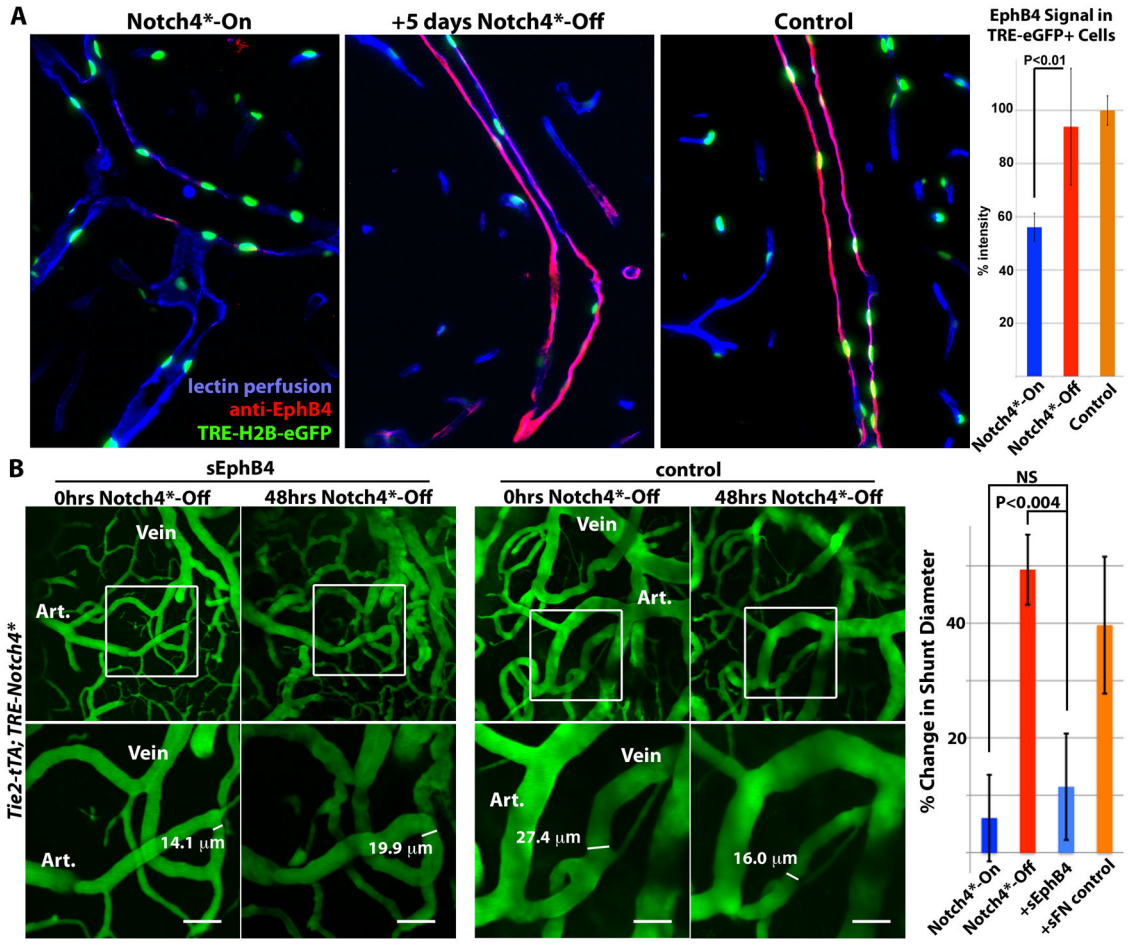

Figure 5. Venous marker EphB4 is re-expressed in venous endothelial cells and required for AV shunt regression

(A) Sagittal sections showing veins in the cerebellum of *Tie2-tTA; TRE-Notch4*; TRE-H2B-eGFP* mutants before and 5 days after Notch4* repression, with littermate *Tie2-tTA; TRE-H2B-eGFP* control. EphB4 expression in TRE-eGFP+ cells, by immuno-fluorescence staining, was selectively reduced in Notch4* expressing mutant, and recovered upon Notch4* repression. Graph shows quantification of EphB4 fluorescence signal intensity in TRE-GFP+ cells. *n*=4 for mutants, n=3 for controls, an average of ~12 cells per vessel and >5vessels per mouse. (B) Two-photon timelapse imaging of cortical brain vessels through a cranial window in *Notch4** mutant mice. Plasma was labeled by intravenous FITC-dextran. Treating *Notch4** mutant mice with soluble EphB4 (sEphB4) inhibited the regression of the AV shunt examined over 48hrs of *Notch4** repression. In a littermate *Notch4** mutant treated with control soluble human fibronectin (sFN), the AV shunt was reduced in diameter following 48hrs of *Notch4** repression. Quantification of changes in minimal AV shunt diameter over 48hrs in mice without repression of *Notch4** (*Notch4**-On, *n*=35 AV shunts in 11 mice), with repression of *Notch4** (*Notch4**-Off, *n*=22 AV shunts in 10 mice), with repression of *Notch4** and sEphB4 intravenous treatment (+sEphB4, *n*=26 AV shunts in 5 mice), and with repression of *Notch4** and sFN control intravenous treatment (+sFN control, *n*=13 AV shunts in 2 mice). Error bars represent s.e.m. between individual AV shunts.

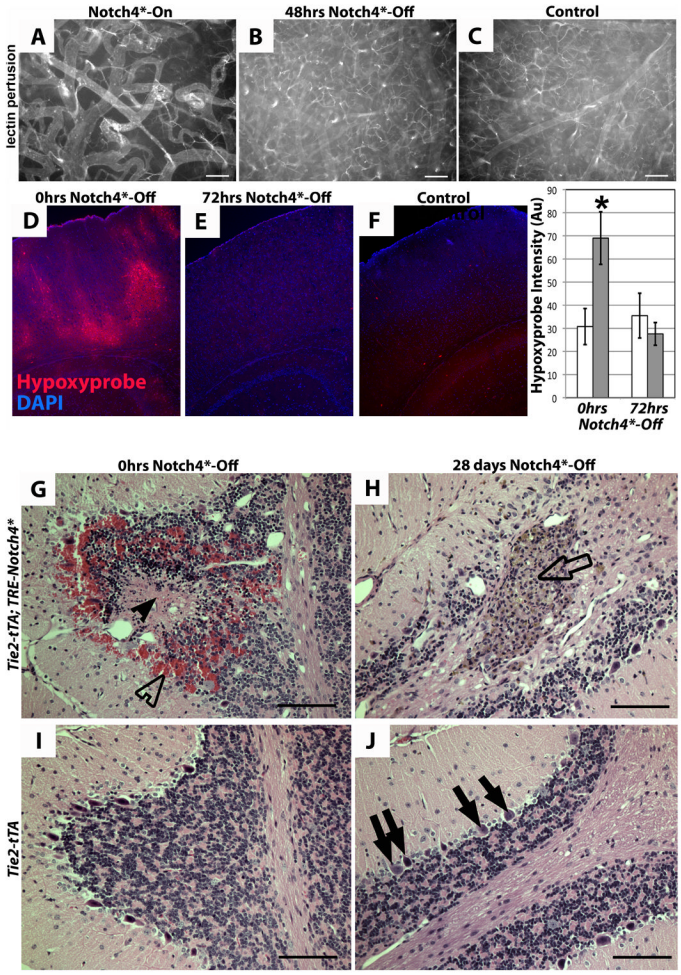

Figure 6. Repression of *Notch4 normalizes vascular perfusion, oxygenation, tissue structure**

(A–C) Vascular perfusion of surface vessels of the cerebral cortex by fluorescent tomato-lectin. Following repression of *Notch4**, capillary perfusion was increased. (D–F) Immunofluorescence (red) staining for hypoxyprobe (pimonidazole) adduct in coronal section of mouse cortex. Patches of staining were visible in mutant mice with neurologic defects before *Notch4** suppression (D). Staining was reduced 72hrs after suppression of *Notch4** (E). Control tissue shows an absence of staining (F). Quantification of staining intensity in cortical brain relative to non-specific IgG controls (*P<0.05 vs. all other groups). *n*=9 at 0hrs *Notch4**-Off, *n*=8 at 24hrs *Notch4**-Off. (G–J) Hematoxylin and eosin staining of sagittal paraffin sections of cerebellum. In *Notch4**- mutant prior to *Notch4** repression (0hrs *Notch4**-Off), areas of hemorrhage (open arrowhead) and necrotic tissue (closed arrowhead) were visible (G). After 28 days of *Notch4** suppression (*Notch4**-Off), areas of scarring were visible (open arrow), but hemorrhage and necrotic tissue had been resolved (H). The numbers of purkinje cells were decreased in H when compared to these cells in the corresponding area in control J (solid arrows). Granular cells (open arrow in H) were found in the scarred area. Scale bar = 100μm.

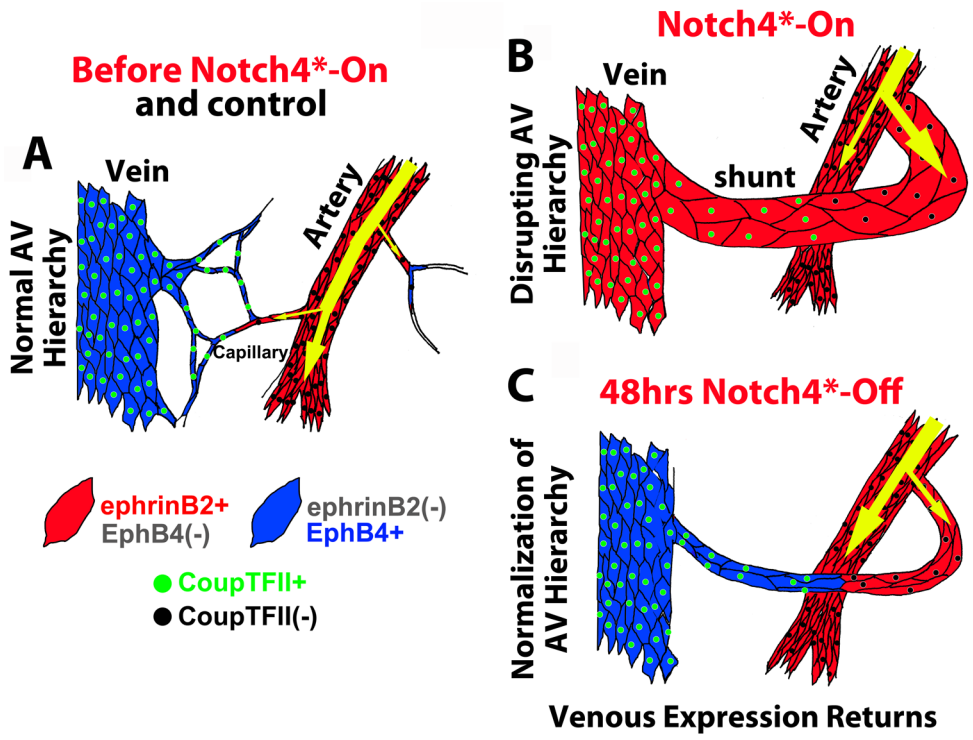

Figure 7. Model for AVM regression: normalization of arteriovenous programming elicited by repression of *Notch4 initiates AVM narrowing**

(A) In control mice, Notch and ephrin-B2 are expressed in arteries and into capillaries. Coup-TFII and EphB4 are expressed in veins, and into capillaries. (B) In mutant mice, *Notch4** is forcibly expressed throughout the endothelium, causing the repression of EphB4, and the expression of ephrin-B2 through AV shunts. The venous marker Coup-TFII, upstream of Notch, is retained, demarcating the original arterial venous boundary. (C) Repression of *Notch4** allows EphB4 to be re-expressed in Coup-TFII+ venous segment. Normalization of Ephrin-B2/EphB4 signaling in the AV cell interface results in reorganization of endothelial cells, initiating the AV shunt narrowing and AVM regression.